Journal of Fluorescence, Vol. 12, Nos. 3/4, December 2002 (© 2002)

Synthesis, Characterization, and Luminescence Spectroscopic Accessibility Studies of *tris*(2,2′-Bipyridine)Ruthenium(II)-Labeled Inorganic-Organic Hybrid Polymers

Elisabeth Holder,[1] Dieter Oelkrug,[2] Hans-Joachim Egelhaaf,[2] Hermann A. Mayer,[1] and Ekkehard Lindner[1,3]

May 14, 2002; accepted June 19, 2002

The modified *tris*(2,2′-bipyridine)ruthenium(II) complex **2** was anchored via a sol-gel process to different polysiloxane matrices to give a series of novel inorganic–organic hybrid polymers. One of the bipyridine ligands of **2** was provided with a long-chain spacer carrying a triethoxysilyl function (T group) at the end, which enables almost free mobility of the transition metal center. The polymers were swollen in several organic solvents of different polarity to investigate the luminescence behavior in the presence of quencher molecules. The luminescence of **2** was quenched using anthracene and atmospheric oxygen in appropriate concentrations of $5 \cdot 10^{-4}$ to $5 \cdot 10^{-3}$ and $3 \cdot 10^{-3}$ M, respectively. The luminescence behavior of **2** was determined by steady-state and time-resolved luminescence experiments. Translational mobilities of molecular species dissolved in the liquid phase were investigated by the kinetics of luminescence quenching after laser excitation. Both the translational mobility of anthracene and atmospheric oxygen, specified with the rate constant k_2 and the percentage of accessible luminescent centers were determined. Translational mobilities and the accessibility for anthracene and atmospheric oxygen in hybrid materials are significantly higher than in conventional Q type polysiloxanes.

KEY WORDS: Inorganic-organic hybrid polymers; tethered ruthenium complex; luminescence quenching; reduced accessibility; diffusion coefficients.

INTRODUCTION

Sol-gel processed polysiloxanes [1] have been widely investigated as potential matrices for reporter molecules in chemical sensors [2,3]. More recently, they have also received attention as catalyst supports, for example, for enzymes and catalytically active transition metal complexes [4,5]. Upon swelling of the polymer in appropriate solvents, an interphase is formed, in which solid and liquid phase interpenetrate on a molecular level without forming a homogeneous phase. Ideally, these materials combine the convenient handling of solids with the molecular dispersity of the active sites encountered in homogeneous solutions. Real samples suffer from several problems, among which chemical stability and accessibility of the active centers are the most serious ones. Decomposition of the matrix is reduced as a result of increased cross-linking of the polymer, that is, by using T- or Q-functionalized silanes. Leaching of the active centers is

[1] Institut für Anorganische Chemie der Universität Tübingen, Auf der Morgenstelle 18, D-72076 Tübingen, Germany.
[2] Institut für Physikalische und Theoretische Chemie der Universität Tübingen, Auf der Morgenstelle 8, D-72076 Tübingen, Germany.
[3] To whom correspondence should be addressed. Tel.: +49 7071 2972039. Fax: +49 7071 295306. e-mail: ekkehard.lindner@uni-tuebingen.de

1053-0509/02/1200-0383/0

impeded by covalently binding them to the matrix via long-chain T-silyl functionalized spacers and by the employment of polyfunctionalized ligands. However, by increasing the cross-linking of the material, the swelling of the polymer in liquids is reduced, which leads to diffusion problems and to markedly reduced accessibilities of the active centers for the reactants dissolved in the mobile phase. A possible approach to solve this dilemma is the use of hybrid polymers [4] instead of pure polysiloxanes. These hybrid polymers are prepared by subjecting the functionalized silanes **2** (Schemes 1 and 2) to the sol-gel process together with the co-condensation agents **3, 4, 5, 6** and **7** (Scheme 2). The siloxane groups provide the desired degree of cross-linking, while the organic substituents of the co-condensation agents are supposed to enhance the swelling ability of the hybrid polymers.

The intention of this study is the optimization of organically modified polysiloxanes as supports for tethered transition metal complexes, which are employed as catalysts in the hydrogenation or hydroformylation of unsaturated organic substrates. The turnover numbers of catalytic reactions in heterogeneous systems are decreased compared to homogeneous systems because the reaction rates are not only determined by the activity of the complex itself but also by its accessibility for the organic and gaseous reactants.

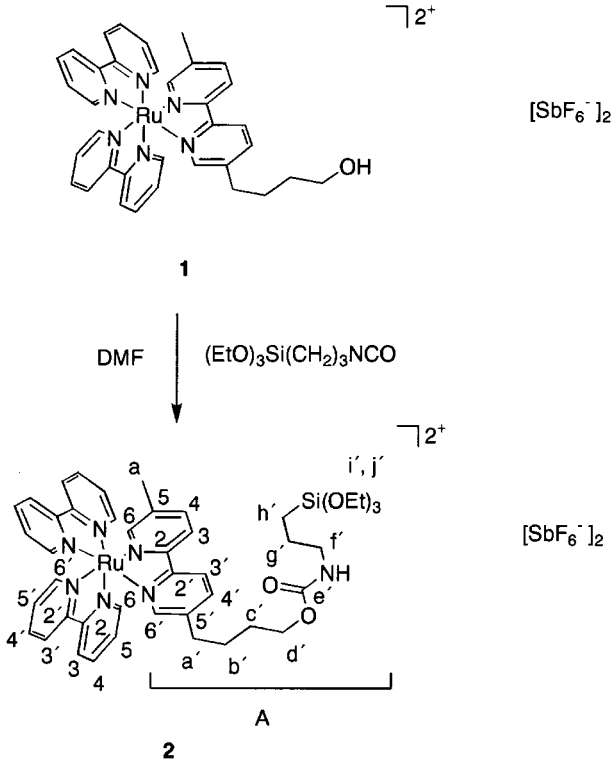

Scheme 1

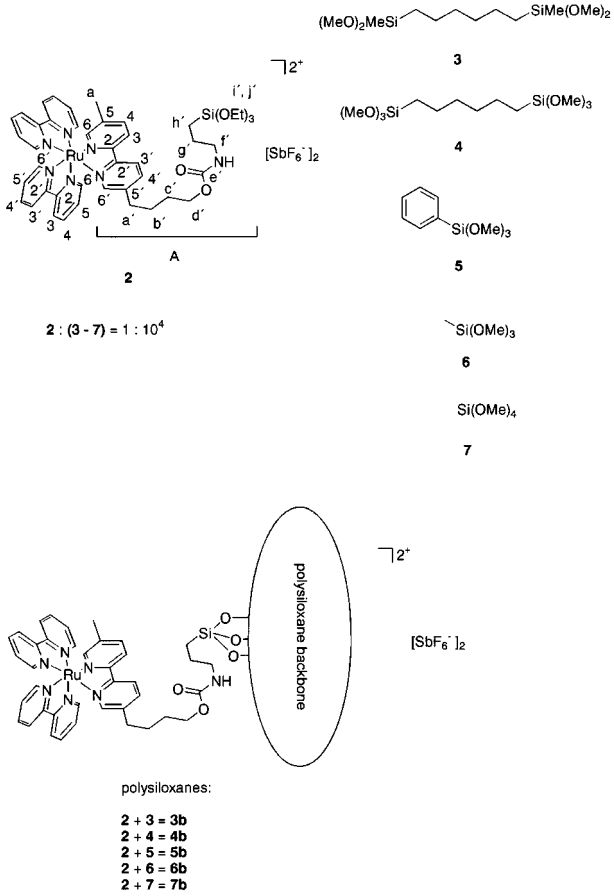

Scheme 2

A variety of spectroscopic techniques, including NMR and UV/Vis spectroscopy, have been applied to determine the accessibilities and mobilities of reactive centers in polymeric phases. NMR spectroscopy provides mainly information on the polymeric matrix and highly concentrated active centers [6,7]. For the investigation of species present in the mobile phase at low concentrations, the highly sensitive UV/Vis luminescence spectroscopy is more appropriate. Ample use has been made of luminescent probes to characterize the microenvironment in sol-gel processed materials [8–23]. The vast majority of these publications deals with probe molecules sequestered within the matrix, whereas only relatively few studies employ covalently attached probes [22,24–37].

Complexes of the ruthenium(II)-polypyridine family have attracted great attention as luminescent probes, mainly in oxygen-sensing devices [38]. Light absorption by $[Ru(bpy)_3]^{2+}$ results in the Franck-Condon singlet metal to ligand charge transfer (^{1}MLCT) excited state, which undergoes subpicosecond intersystem crossing to a long-lived ^{3}MLCT excited state $^1R \xrightarrow{h\nu} {}^1R^* \rightarrow {}^3R^*$

[39,40]. The triplet state decays by non-radiative deactivation and luminescence. Because of their long lifetimes, ^{3}MLCT excited states are quenched efficiently by electron or energy transfer to appropriate molecules, such as dioxygen and anthracene [41–44]. Energy transfer takes place by an electron exchange mechanism [45] upon close contact of **2** and the quencher molecules, according to the reactions $^3R^* + {}^3O_2 \rightarrow {}^1R + {}^1O_2$ and $^3R^* + {}^1A \rightarrow {}^1R + {}^3A$ (Schemes 3 and 4).

In this work we investigate the bimolecular quenching of the long-lived luminescence of the ruthenium(II) complex **2** by energy transfer to dioxygen, as well as anthracene. The ruthenium complex serves as a model compound for catalytically active complexes; the quenchers used in our study represent the organic and gaseous substrates of catalytic processes. The ruthenium complex is either dissolved in solution **1,** or covalently bound to the siloxane polymers **3b–7b** (see Scheme 2). The polymers are suspended in a series of different liquids. The kinetic analysis of the time-resolved luminescence quenching experiments provides a detailed picture how the accessibility of matrix-bound transition metal catalysts is affected by the structure of the polymer, the type of solvent, and the size of the reactant dissolved in the liquid phase. The insight thus gained will be useful in the design of new polysiloxane matrices for transition metal complex catalysed hydrogenations and hydroformylations with enhanced reaction rates.

EXPERIMENTAL

Syntheses

Elemental analyses were carried out on a Vario EL analyser (Fa. Elementar Analytische Systeme, Hanau).

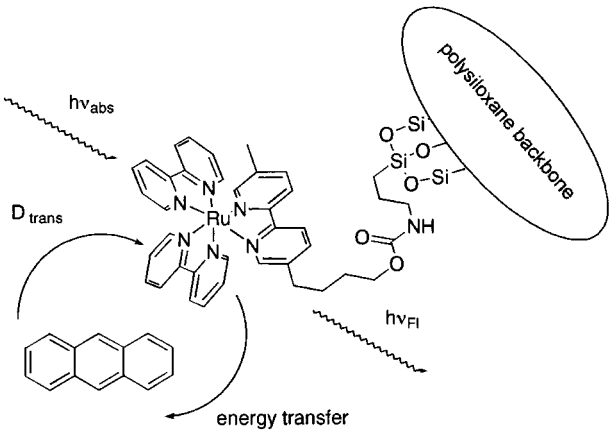

Scheme 3

Solution nuclear magnetic resonance spectra (NMR) were recorded on a Bruker DRX 250 spectrometer at 298 K. Frequencies and standards were as follows: ^{1}H NMR, 250.13 MHz; ^{13}C{^{1}H} NMR, 62.90 MHz. All NMR spectra were calibrated relative to partially deuterated solvent peaks, which are reported relative to tetramethylsilane (TMS). EI mass spectra were acquired on a Finnigan TSQ 70 instrument and are reported as mass/charge (*m*/*z*). Infrared data were obtained on a Bruker IFS 48 FT-IR spectrometer. SEM micrographs were recorded on a Zeiss DSM 962 with a tungsten cathode (4.5 nm diameter); BET surfaces and pore volumes were obtained with a Coulter SA3100 (Beckman Coulter GmbH), measuring the adsorption and desorption isotherms after drying the samples for 12 hr at T = 50°C under vacuum.

CP/MAS solid-state NMR spectra were recorded on Bruker DSX 200 (4.7 T) (^{29}Si) and ASX 300 (7.05 T) (^{13}C) multinuclear spectrometers equipped with widebore magnets. Magic angle spinning was applied at 3.5 kHz (^{29}Si) and 10 kHz (^{13}C), respectively. All samples were packed under exclusion of molecular oxygen. Frequencies and standards: ^{29}Si, 39.75 MHz (Q_8M_8, relative to TMS); ^{13}C, 75.47 MHz [TMS, carbonyl resonance of glycine (δ 170.09) as the second standard]. No relative intensities are given for ^{29}Si NMR spectra, because of the different efficiencies of magnetization transfer to inequivalent ^{29}Si nuclei.

All manipulations were performed under an atmosphere of dry argon by employing usual Schlenk techniques. The solvents were dried according to common methods, distilled, and stored under argon. Complex **1** [46] and the co-condensation agents **3** [47] and **4** [48] were synthesized according to literature methods. Compounds **5, 6**, and **7** were purchased from Fluka.

Preparation of Complex 2

The orange [*bis*(2,2-bipyridyl)(5-(4-hydroxybutyl)-5′-methyl-2,2′-bipyridyl)-ruthenium(II)]-*bis*(hexafluoroantimonate) (**1**) (0.71 g, 0.629 mmol) was dissolved in 25 mL of DMF. A solution of triethoxysilyl(propyl)isocyanate (155 μL, 0.629 mmol) in 5 mL of DMF was added dropwise. The mixture was stirred for 48 hr at 130°C until a red solution was formed. The volatile components of the solution were removed in vacuum, and the residual red solid complex was purified by column chromatography (acetone, neutral, and water-free aluminum oxide column, length: 4 cm, diameter: 2 cm). The solvent was removed under reduced pressure, and the resulting red solid was washed with 10 mL of *n*-hexane: yield 0.78 g (90.1 %); ^{1}H NMR (CD_2Cl_2): δ 0.55 (m, 2H, h′), 1.13 (m, 2H, j′), 1.31–1.47 (m, 4H, c′, b′), 2.18

(s, 3H, a), 2.46 (m, 2H, g′), 2.75–2.84 (m, 2H, a′), 3.03 (m, 2H, f′), 3.72 (m 6 H, i′), 3.97 (m, 2H, d′), 7.31–7.36 (m, 5H, bpy-5,5′, 6′A), 7.79 (m, 5H, bpy-6,6′, 6A) 7.87–7.92 (m, 2H, 4A, 4′A), 7.96 (s, NH), 8.02–8.19 (m, 4H, bpy-4,4′), 8.19–8.22 (m, 2H, 3A, 3′A), 8.36–8.39 (m, 4H, bpy-3,3′); $^{13}C\{^1H\}$ NMR (CD_2Cl_2): δ 6.8 (Ch′), 14.9 (Cg′), 18.5 (Cj′), 18.8 (Ca), 19.5 (Cb′), 34.6 (Cc′), 36.3 (Ca′), 45.5 (Cf′), 58.8 (Ci′), 60.2 (Cd′), 124.4 (C3,3′), 124.6 (bpy-C3,3′), 128.4 (bpy-C5,5′), 138.4 (bpy-C4,4′), 139.9 (C4A, 4′A), 145.5 (C5A, 5′A), 150.9, 151.0 (C6A, 6′A), 151.7 (bpy-C6,6′), 155.5, 155.6 (C2A, 2′A), 157.2 (bpy-C2,2′); 160.0 (Ce′). FD-MS *m/z* 451.5 [M^{2+}], 1140.75 [M^+]. Anal. Calcd for $C_{45}H_{55}N_7O_5SiRuSb_2F_{12}$: C, 39.32; N, 7.13; H, 4.03. Found: C, 39.31; N, 7.77; H, 4.57%.

*Sol-Gel Processing of **2** with Different Co-condensation Agents: General Procedure*

The T-silane **2** was polycondensed with the co-condensation agents **3, 4, 5, 6**, and **7** (see Scheme 2) in a molar ratio of 1 : 10^4. A mixture of the respective T^0- and D^0-functionalized monomeric silanes with water, methanol/THF (1/5, v/v), and $(n\text{-Bu})_2Sn(OAc)_2$ as catalyst was stirred for 12 hr at 30°C until the gels precipitated. Subsequently the solvent was removed under reduced pressure, and the resulting gels were dried for 4 hr *in vacuo*. Solvent processing was performed by vigorously stirring the large gel particles in 10 mL of *n*-hexane overnight. The wet gels were triturated and washed twice with 20 mL of *n*-hexane and dichloromethane and dried *in vacuo* for 4 hr. Prior to luminescence measurements the samples were aged artificially for 1 week at 90°C to obtain highly cross-linked samples that do not significantly change between preparation and completion of the NMR, BET, and luminescence measurements.

*Preparation of the Polysiloxane **3b***

A mixture of **2** (0.6 mg, $4.36 \cdot 10^{-4}$ mmol), **3** (1.45 g, 4.99 mmol), 1 mL of methanol, 5 mL of THF, 500 μL of water, and $(n\text{-Bu})_2Sn(OAc)_2$ (25 mg, 0.073 mmol) was sol-gel processed: yield 0.86 g (59.3 %); ^{13}C CP/MAS NMR δ 50.2 ($SiOCH_3$), 33.6 ($Si(CH_2)_2CH_2CH_2$-$(CH_2)_2Si$), 23.5 ($SiCH_2CH_2(CH_2)_2CH_2CH_2Si$), 18.1 ($SiCH_2(CH_2)_4CH_2Si$), −0.1 ($SiCH_3$); ^{29}Si CP/MAS NMR (silicon substructure) δ −11.7 (D^1), −22.4 (D^2). Anal. Calcd for $C_{45}H_{55}N_7O_5SiRuSb_2F_{12}(C_8H_{18}O_2Si_2)_{10000}$: C, 47.40; H, 8.93, Found: C, 47.30; H, 8.86%. BET surface A_{BET} = 1.25 m^2/g.

*Preparation of the Polysiloxane **4b***

A mixture of **2** (0.90 mg, $6.54 \cdot 10^{-4}$ mmol), 4 (1.63 g, 4.99 mmol), 1 mL of methanol, 5 mL of THF, 500 μL of water, and $(n\text{-Bu})_2Sn(OAc)_2$ (25 mg, 0.073 mmol) was sol-gel processed: yield 0.91 g (55.83 %); ^{13}C CP/MAS MNR δ 50.4 ($SiOCH_3$), 33.3 ($Si(CH_2)_2CH_2CH_2$-$(CH_2)_2Si$), 23.2 ($SiCH_2CH_2(CH_2)_2CH_2CH_2Si$), 13.0 ($SiCH_2(CH_2)_4CH_2Si$); ^{29}Si CP/MAS NMR (silicon substructure) δ −58.5 (T^2), −67.5 (T^3). Anal. Calcd for $C_{45}H_{55}N_7O_5SiRuSb_2F_{12}(C_6H_{12}O_3Si_2)_{10000}$: C, 38.25; H 6.40 Found: C, 37.10; H, 6.85%. BET surface A_{BET} = 21.18 m^2/g.

*Preparation of the Polysiloxane **5b***

A mixture of 2 (1.8 mg, $1.31 \cdot 10^{-3}$ mmol), 5 (2.01 g, 10.13 mmol), 1 mL of methanol, 5 mL of THF, 500 μL of water, and $(n\text{-Bu})_2Sn(OAc)_2$ (25 mg, 0.073 mmol) was sol-gel processed: yield 0.96 g (47.76 %); ^{13}C CP/MAS NMR δ 134.5, 130.7, 127.9 (aromatic ring); ^{29}Si CP/MAS NMR (silicon substructure) not measurable. Anal. Calcd for $C_{45}H_{55}N_7O_5SiRuSb_2F_{12}(CH_3O_{1.5}Si)_{10000}$: C, 55.59; H, 3.89. Found: C, 50.06; H, 3.18%. BET surface A_{BET} = 2.08 m^2/g.

*Preparation of the Polysiloxane **6b***

A mixture of **2** (1.7 mg, $1.23 \cdot 10^{-3}$ mmol), **6** (1.36 g, 9.98 mmol), 1 mL of methanol, 5 mL of THF, 500 μL of water, and $(n\text{-Bu})_2Sn(OAc)_2$ (25 mg, 0.073 mmol) was sol-gel processed: yield 0.49 g (36.02 %); ^{13}C CP/MAS NMR δ 49.8 ($SiOCH_3$), −3.1 ($SiCH_3$); ^{29}Si CP/MAS NMR (silicon substructure) δ −56.8 (T^2), −65.3 (T^3). Anal. Calcd for $C_{45}H_{55}N_7O_5SiRuSb_2F_{12}$-$(C_6H_5O_{1.5}Si)_{10000}$: C, 18.24; H 4.48 Found: C, 17.01; H, 4.86%. BET surface A_{BET} = 3.51 m^2/g.

*Preparation of the Polysiloxane **7b***

A mixture of **2** (1.30 mg, $9.45 \cdot 10^{-4}$ mmol), **7** (1.56 g, 10.24 mmol), 1 mL of methanol, 5 mL of THF, 500 μL of water, and $(n\text{-Bu})_2Sn(OAc)_2$ (25 mg, 0.073 mmol) was sol-gel processed: yield 0.99 g (63.46 %); ^{29}Si CP/MAS NMR (silicon substructure) δ −110 (Q^4), −101 (Q^3). Anal. Calcd for $C_{45}H_{55}N_7O_5SiRuSb_2F_{12}(O_4Si)_{10000}$: C, 0.76; H 0.07 Found: C, 9.47; H, 2.13%. BET surface A_{BET} = 4.89 m^2/g.

Luminescence Measurements

For the measurements of the hybrid polymers the powders (3.0–4.0 mg) were suspended in 3 mL of the

respective liquid. The suspensions were vigorously stirred with a magnetic stirrer to avoid sedimentation. The temperature during the measurements was kept constant at T = 293 K. For quenching experiments, anthracene in concentrations of $c = 5 \cdot 10^{-4} - 5 \cdot 10^{-3}$ M was dissolved in the liquid phase. Air-saturated liquids contained about $c \approx 2 \cdot 10^{-3}$ M of dioxygen. The employed molar ratio of 10^{-4} between **2** and the co-condensation agents **3–7** corresponded to a local concentration of **2** in the polysiloxane matrix of $c \approx 4 \cdot 10^{-4}$ M.

Steady-state luminescence and luminescence excitation spectra were obtained on a SPEX Fluorolog 222 fluorometer, equipped with Glan-Thompson polarizers. Luminescence spectra were corrected for the sensitivity of the photomultiplier tube and luminescence excitation spectra for the quantum flux of the exciting light.

Luminescence decay curves were acquired by the single-photon counting method. A picosecond diode laser (PICO QUANT GmbH, Berlin, Model LDH 400) was used for excitation (wavelength 392 nm) and a R928 photomultiplier tube (Hamamatsu) for detection. The signal from the photomultiplier tube was fed into a multichannel analyser via a picosecond amplifier/discriminator and a time to amplitude converter (EG&G ORTEC). The time resolution of this setup is limited to decay times of $\tau \geq 0.5$ ns.

RESULTS

Synthesis of the T-silyl Functionalized *tris*(2,2′-Bipyridine)Ruthenium (II) Complex 2

To furnish the starting material **1** [46] with a spacer unit equipped with a terminal T-silyl function, a solution of triethoxysilyl(propyl)isocyanate in DMF was added in a molar ratio (see Scheme 1). An addition reaction takes place, binding the spacer with its isocyanate substituent to the hydroxy group of the 5-(4-hydroxybutyl)-5′-methyl-2,2′-bipyridine moiety of **1**. After column chromatographic purification, **2** represents a red solid, which is sensitive to moisture and dissolves readily in organic solvents of high polarity because of its ionic character. The composition of **2** was verified by an EI mass spectrum showing the expected molecular peak. ^{1}H and ^{13}C{^{1}H} NMR spectra of **2** reveal the expected resonances. Detailed analytical data are summarized in the Experimental Section.

Synthesis of the Polymeric tris(2,2′-Bipyridine)Ruthenium(II) Complexes 3b-7b

When tris(2,2′-bipyridine)ruthenium(II) is used as luminescent label in stationary phases, it should be present in highly diluted concentrations, to avoid aggregation of the luminophores. Therefore the sol-gel process of **2** was carried out in the presence of high amounts (1:10^4) of the mono- and bifunctional co-condensation agents **3, 4, 5, 6**, and **7** (see Scheme 2) influencing the properties of the resulting polymeric materials essentially. The properties of sol-gel processed materials strongly depend on the applied reaction conditions such as concentration of the starting materials, amount and type of solvent, temperature, reaction time, drying conditions of the wet gel, and type of catalyst. To ensure the same reaction kinetics for the synthesis of each polymer as a prerequisite for comparable results, the adherence to uniform reaction conditions must be maintained during the entire hydrolysis and polycondensation procedure [4,46–48]. THF/Methanol (1/5 v/v) was added during the sol-gel process to homogenise the reaction mixture. (*n*-Bu)$_2$Sn(OAc)$_2$ is an appropriate catalyst, and do not interfere with 2 [49].

The ^{29}Si and ^{13}C CP/MAS NMR spectra of the polymers **3b–7b** ($y = 10^4$, see Scheme 2) are dominated by the signals of the building blocks **3–7**. Hence no ^{29}Si signals for the polycondensed T^n functions of **2** are observed. In the case of **3b** two very small signals are observed for D^0- and D^1- silyl species, and an intense resonance occurs for the nearly complete hydrolysed co-condensation agent. The ^{29}Si CP/MAS NMR spectrum of **4b** reveals resonances for T^2- and T^3- silyl groups, in which the T^2 signal is more intense than that of T^3. This observation is in agreement with former results and points to a medium cross-linkage of the polymer. Both spectra are similar to those of the recently reported unlabeled hybrid polymers **D^i-C$_6$-D^i** and **T^m-C$_6$-T^m** [6,49]. Because of the long distance to the next protons the ^{29}Si CP/MAS NMR spectrum of **5b** was not measurable. In the case of polymer **6b** the ^{29}Si CP/MAS NMR spectrum is characterized by two resonances of different intensities, and are assigned to T^2 (small) and T^3 (intense) silyl species. The ^{13}C CP/MAS NMR spectra of the stationary phases **3b, 4b**, and **7b** show resonances at δ 50.0, attributed to the carbon atoms of the silicon bound methoxy groups. Because of steric effects the portion of non-hydrolyzed methoxy residues is higher in the case of polymer **4b** than in the other polymers.

Scanning Electron Micrographs

The scanning electron micrographs of the polymers **3b–7b** show irregularly shaped particles with broad size distributions, the diameters ranging from several hundred nanometers to some 10 μ*M*. The Q type polymer **7b** shows the sharp edges and conchoidal fractures typical

for brittle, amorphous materials. The same is true for the hybrid polymers **3b, 4b**, and **6b** (Fig. 1).)

In samples of polymer **6b**, fibers, whose diameters are between some 100 nm and some 1 μ*M*, accompany the irregular particles. In polymer **5b**, particles of nearly globular shapes are observed, which have connecting fibers with diameters of some 10–100 n*M*. Obviously polymers **3b, 4b**, and **7b** form three-dimensional networks, whereas in polymers **5b** and **6b** considerable fractions of low-dimensional structures are found.

Luminescence Spectroscopic Investigations

*Luminescence and Luminescence Excitation Spectra of **1***

Figure 2 presents the UV/Vis absorption and luminescence spectra of the ruthenium complex **1** [46] in acetonitrile solution. The maxima of the ^{1}MLCT absorption and ^{3}MLCT luminescence bands of **1** are found at $\tilde{\nu}_{abs}^{MLCT} = 22000\ cm^{-1}$ and $\tilde{\nu}_{em}^{max} = 15700\ cm^{-1}$, respectively. These spectral positions are very similar to those observed for the unsubstituted *tris*(2,2′-bipyridine)ruthenium(II) complex ($\tilde{\nu}_{abs}^{MLCT} = 22000$ and $\tilde{\nu}_{em}^{max} = 16600\ cm^{-1}$) [50]. Whereas the ^{1}MLCT absorption band does not show a noticeable solvent dependence, the spectral positions of the luminescence maxima vary significantly, due to the differences in stabilization of the ^{3}MLCT excited state by the various solvents [51]. In methanol, acetone, and acetonitrile the luminescence maxima are found at approximately $\tilde{\nu}_{em}^{max} = 15700\ cm^{-1}$, while in THF the maximum is red-shifted by $\Delta\tilde{\nu} = 200\ cm^{-1}$. In DCM, where the luminescence spectrum is remarkably structured, the maximum is observed at $\tilde{\nu}_{em}^{max} = 16300\ cm^{-1}$ (Table 1). Upon co-polycondensation of the T-silyl functionalized ruthenium complex **2**

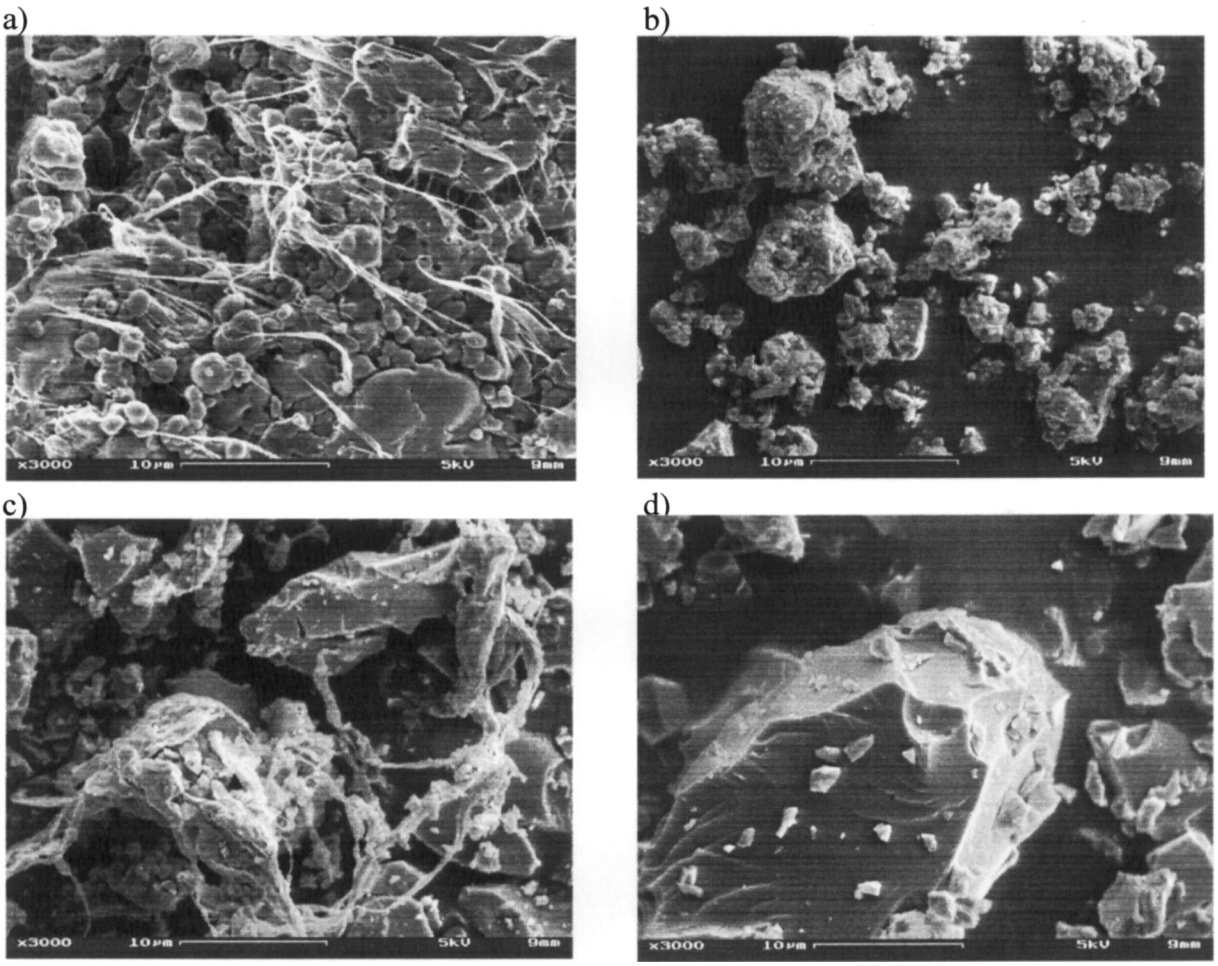

Fig. 1. Scanning electron micrographs of polymers **5b** (a), **7b** (b), **6b** (c), and **3b** (d). The samples have been sputtered with carbon. Magnification 3000 fold, acceleration voltage U = 5 kV.

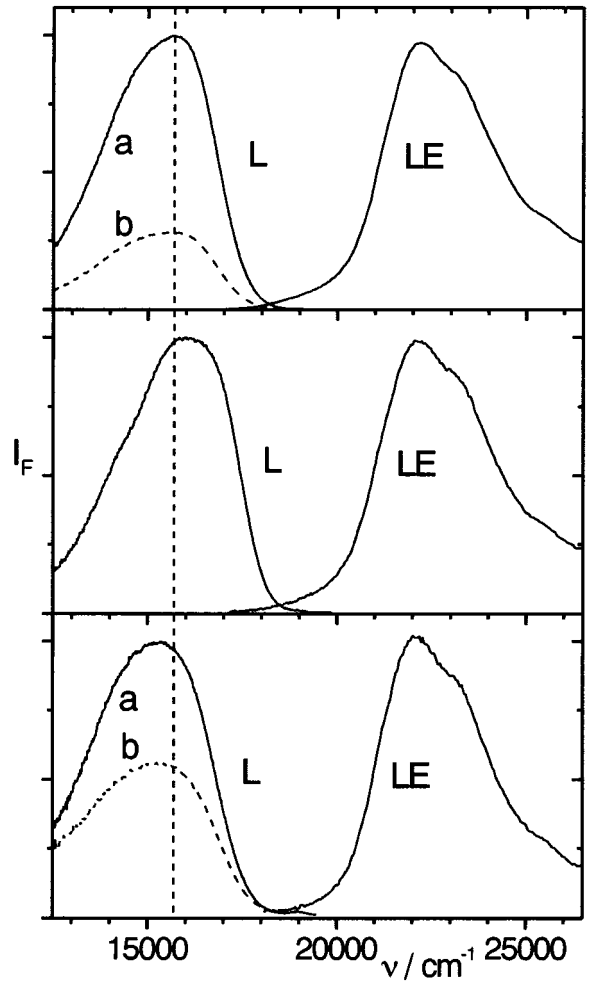

Fig. 2. Luminescence (L) and luminescence excitation spectra (LE) of **1** in acetonitrile solution (top panel), of **7b** (middle panel) and **3b** (bottom panel), both polymers suspended in acetonitrile, (a) under nitrogen atmosphere, (b) quenched by anthracene. Excitation at $\tilde{\nu}$ = 22000 cm^{-1}, luminescence observed at $\tilde{\nu}$ = 15700 cm^{-1}.

with the silanes **3–7** and swelling the resulting polymers **3b–7b** (see Scheme 2) in different solvents, the spectral positions of the luminescence maxima undergo slight, but noticeable changes against the values observed for **1** in solution. The spectral shifts correlate with the extent of solvation of the ruthenium complexes by the liquids. In Q type materials, the luminescence maxima are located at $\tilde{\nu} \approx 16000$ cm^{-1} (see Fig. 2), independent of the solvent (Table 1). This blue-shift, $\Delta\tilde{\nu} = 500$ cm^{-1} vs. the position in solution in the case of THF, is due to the rigidity of the immediate environment of the luminescence probe, that is, the absence of significant solvent relaxation during the excited state lifetimes of the ruthenium complex [51]. In the swollen hybrid polymers **3b–6b**, efficient solvent relaxation is observed, that is, the luminophores are well solvated by the solvent molecules, whose mobility is comparable to that in bulk liquids [52]. Thus, in the suspended polymer **4b,** the spectral positions are very close to those in homogeneous solutions. In **3b, 5b,** and **6b** the luminescence maxima are red shifted by $\Delta\tilde{\nu} \approx 100 - 500$ cm^{-1} compared to the spectral positions of **1** in solutions of the respective solvents (Fig. 2). However, in the case of **5b** in methanol, where the solvent does not wet the polymer, the luminescence maximum is slightly blue shifted against solution.

Table I. Spectral Positions of the Luminescence Maxima ($\tilde{\nu}$ in cm^{-1}) of **1** in Solutions and of **2** in Polymers **3b–7b**, Suspended in a Series of Liquids

Sample Solvent	**3b**	**4b**	**5b**	**6b**	**7b**	**1**
MeOH	15300	15710	15750	15490	16040	15740
MeCN	15300	15650	15330	15410	15970	15695
Acetone	15270	15650	15360	15490	16050	15730
THF	15090	15650	15240	15360	16010	15510
DCM	15380	16050	15480	15500	16020	16330

Kinetic Analysis of Luminescence Decay Curves

An ideal interphase represents a solution-like state. With the simple assumption of such an ideal interphase, the deactivation rate $-d[R^*]/dt$ of photoexcited ruthenium(II) complexes can be described by conventional kinetics for homogeneous systems (Scheme 4):

$$-\frac{d[R^*]}{dt} = (k_1 + k_q \cdot [S]) \cdot [R^*] \qquad (1)$$

Here [R*] is the concentration of excited ^{3}ruthenium complexes in the materials **1** and **3b–7b,** and [S] is the concentration of a potential reactant that is dissolved in the mobile liquid compound of the interphase. The rate constant k_1 describes spontaneous deactivation of R* to the inactive electronic ground state, and k_q the deactivation by interaction with S. The larger k_q, the more mobile S is in the interphase. As model reaction we chose intermolecular transfer of excitation energy accompanied by double spin flip, namely:

$$^3R^* + {}^1anthracene \rightarrow {}^1R + {}^3anthracene^* \qquad (2)$$

$$^3R^* + {}^3O_2 \rightarrow {}^1R + {}^1O_2^* \qquad (3)$$

These reactions are possible only by an exchange mechanism after close contact between ^{3}R* and S or after formation of an exciplex ^{1,3}(RS)* see (Scheme 4).

In a pulsed laser experiment followed by single-photon counting of R* luminescence, the concentration

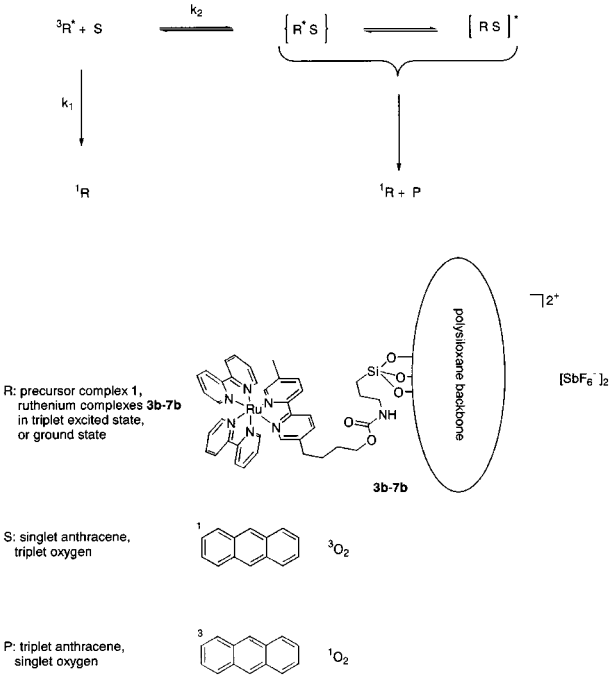

Scheme 4

of R* is always by orders of magnitude lower than that of S, [R*] ≪ [S] ≈ const., so that Eq. (1) can be integrated according to:

$$[R^*] = [R^*]_0 \cdot e^{-(k_1+k_2)t} \tag{4}$$

where $[R^*]_0$ is the concentration of the excited ^{3}ruthenium complexes at t = 0, and $k_2 = k_q\,[S]$. In a semi-logarithmic plot, Eq. (4) should give a straight line of ^{3}ruthenium luminescence intensity vs. time. This behavior is observed for **1** in homogeneous solution over 2–3 intensity decades and a large range of anthracene and oxygen concentrations so that k_2 and—if [S] is known—also k_q can directly be determined from Eq. (4). However, in interphases formed from **3b–7b** with a variety of liquids, almost all quenching experiments yield strongly nonexponential decay curves. To approximately eliminate the contribution of fluctuations in k_1 to nonexponentiality (see sections: *Luminescence Decay Curves of **1** and **3b–7b** in the Presence of Oxygen* and *Luminescence Decay Curves of **1** and **3b–7b** in the Presence of Anthracene as Quenching Substrate)* the decay curves in the presence of S are divided by the decay curves for [S] = 0. As long as Eq. (4) is valid, one obtains for the relative luminescence quenching efficiency at a given time, t, after the laser flash:

$$1 - \frac{[R^*]}{[R^*_{S=0}]} = 1 - e^{-k_2 t} \tag{5}$$

that is, a straight line in the semi-logarithmic presentation. In real systems the curves bend, and very often a constant plateau at t → ∞ is revealed. This type of curve can be approximated with good accuracy by:

$$1 - \frac{[R^*]}{[R^*_{S=0}]} = \alpha \cdot [1 - e^{-k_2 t}] \tag{6}$$

where $0 \le \alpha \le 1$ defines an accessibility factor α, that is, the fraction of excited ^{3}ruthenium complexes that are able to convert S into P, whereas the fraction (1 − α) is non-reactive ($k_2 \to 0$). From the product point of view, the accessibility factor α gives the ratio of actual product yield to the maximum possible product yield at t → ∞:

$$[P_{\max}] = [R^*_0]\,\frac{k_2}{(k_1 + k_2)}$$

$$\alpha = \frac{[P](t \to \infty)}{[P_{\max}](t \to \infty)} = \frac{1 - \dfrac{[R^*]}{[R^*_{S-0}]}}{(1 - e^{-k_2 t})} \tag{7}$$

All time-resolved experiments of this study were evaluated according to Eq. (7).

Luminescence Decay Curves of **1** *and* **3b–7b** *Without Quencher*

The luminescence decay curves of **1** dissolved in low viscous solutions are single exponential with decay times of $\tau_F \approx 750$–950 ns. For suspensions of the labeled polysiloxanes **3b–7b** in all investigated solvents, slightly non-exponential decay curves are observed.

This type of decay curves is best described by narrow distributions of decay times, but can also be fitted by sums of two exponential functions without loss of accuracy. In polymer **7b,** both components are longer lived than the corresponding lifetime of **1** in solution, due to the rigidity of the matrix that reduces non-radiative deactivation rates [51]. For suspensions of **7b** in all liquids, almost identical values of $\tau_1 \approx 1.0$ μs and $\tau_2 \approx 1.8$ μs were found for both short and long components. The same values are obtained in the case of **5b** in methanol, where the solvent does not swell the polymer. In all other cases the polymers **3b–6b** exhibit short lifetime components and are close to the decay time of **1** in the corresponding homogeneous solutions, while the long components vary between $\tau_2 \approx$ 1.1 μs and 1.3 μs, depending on the polymer and the suspending liquid.

The short lifetime component is ascribed to ruthenium complexes, which are solvated by the liquid phase, whereas the long lifetime component is due to complexes with a primary "solvation shell" formed by the rigid polymer network [51].

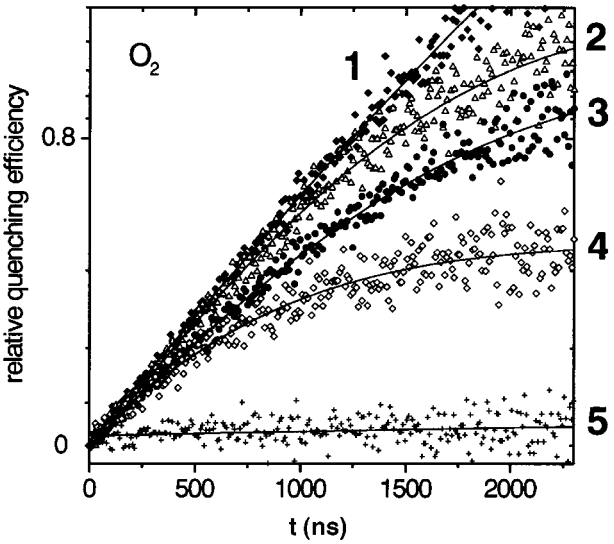

Fig. 3. Relative efficiencies, $1 - \frac{[R^*]}{[R^*]_{S=0}}$, for the quenching of ruthenium luminescence by oxygen. The curves are calculated from the corresponding luminescence decay curves according to Eq. (7). (1) **1** in dichloromethane solution, (2) **5b**, (3) **6b**, (4) **3b**, and (5) **7b**, all polymers suspended in dichloromethane. The concentration of oxygen in the liquid phases is $c(O_2) \approx 2 \cdot 10^{-3}$ M.

Luminescence Decay Curves of **1** *and* **3b–7b** *in the Presence of Oxygen*

Quenching of ruthenium luminescence [53–56] by energy transfer to dioxygen [57] is a bimolecular process requiring close contact between donor and acceptor.

The efficiency of luminescence quenching thus depends on both the mobility of oxygen in the interphase and the accessibility of the transition metal complex. The steady-state luminescence spectra shown in Fig. 2 demonstrate that the quenching efficiency in organically modified polysiloxanes is significantly enhanced compared to unmodified Q type materials. Evaluation of the time-resolved luminescence decay curves according to Eq. (7) yields values for k_2 and α, describing the mobility of oxygen and the fraction of accessible ruthenium complexes (Fig.3 and Table II). In homogeneous solutions of **1**, $\alpha \approx 1$, that is, all ruthenium complexes are equally accessible by oxygen (Figs. 3 and 4). The rate constants k_2 are far below the diffusion controlled limit for all solvents [58]. The ratios between the quenching rate constant k_q, calculated from k_2 and the concentration of oxygen by $k_q = k_2/c[O_2]$, and the rate constants of diffusion k_d, are approximately $\frac{k_q}{k_d} \approx 0.05$ for all solvents, except for dichloromethane, for which $\frac{k_q}{k_d} \approx 0.02$ is found. These values are in close agreement with literature data for $[Ru(bpy)_3]^{2+}$ [58].

In the polymers **3b–7b,** the fraction of accessible ruthenium complexes α varies considerably with both the type of the polymer and the suspending liquid (see Fig. 5). In polymer **7b** only a minor fraction of the tethered complexes is accessible to oxygen, due to the high degree of cross-linking in this material. Polymers **3b** and **4b**, both of which are prepared from bifunctional monomers, behave very similarly with respect to the accessibility by oxygen. The fraction of accessible groups α in these polymers is around 0.5–0.8, the lower values being found in liquids of medium and large dielectric constants. In polymer **6b**, the fraction of accessible complexes is $\alpha \approx 0.9$, regardless of the suspending liquid. In contrast to all other polymers, material **5b** shows a strong dependence of the accessibility on the dispersing solvent. Whereas $\alpha \rightarrow 1$ in less polar solvents like THF, DCM or acetone, in acetonitrile and methanol appropriate values of $\alpha \approx 0.9$ and $\alpha \approx 0.45$ are found. Obviously, the replacement of the methyl group by a phenyl substituent in the silane monomers imparts a strongly hydrophobic nature to the polymer, which impedes its penetration by hydroxylic solvents.

For most polymer/liquid systems, the quenching rate constant k_2 is close to the values observed for **1** in the corresponding solutions (see Table II). This indicates that those ruthenium complexes whose luminescence is quenched by dioxygen are well solvated by the liquid phase.

In cases in which the solvent does not penetrate the polymer (e.g., **5b** in methanol), k_2 is significantly lower than for **1** in solution. For all polymers in DCM, k_2 is slightly larger than the corresponding solution value. This indicates that the factors leading to the unusual low value of $\frac{k_q}{k_d}$ in dichloromethane solution are not fully effective in the polymers. The ruthenium complexes are either not completely solvated by DCM, or the reorientational motions of dichloromethane molecules are impeded by the polymer matrix [52].

In summary, two types of ruthenium complexes can be distinguished in organically modified polysiloxanes. The first type is not accessible to oxygen dissolved in the liquid phase. The luminescence of the second type is quenched by oxygen with rate constants that are close to those obtained for ruthenium complexes dissolved in solvents. In liquids of low and medium polarity, polymer **5b** provides solution-like accessibilities, whereas in highly polar solvents, polymer **6b** shows the best results.

Table II. Quenching Rate Constants, $k_2/10^6 s^{-1}$, and Accessibility Factors, α (in Parentheses), for the Luminescence Quenching by Oxygen ($p(O_2)$ = 0.21 bar) in Solutions of **1** and Suspensions of Polymers **3b–7b** in a Series of Solvents. The Values of k_2 and α Are Obtained by Evaluation of the Corresponding Luminescence Decay Curves According to eq. (7)

Sample Solvent	**3b**	**4b**	**5b**	**6b**	**7b**	**1**
MeOH	4.1 (0.71)	3.8 (0.71)	2.4 (0.45)	3.4 (0.88)	1 (0.03)	3.9 (1)
MeCN	4.2 (0.73)	4.2 (0.71)	3.0 (0.89)	3.9 (0.91)	1.7 (0.10)	4.7 (1)
Acetone	4.1 (0.77)	3.1 (0.83)	3.9 (0.98)	3.6 (0.90)	3.9 (0.06)	4.3 (1)
THF	2.8 (0.53)	2.8 (0.67)	2.8 (0.95)	3.0 (0.85)	1 (0)	3.4 (1)
DCM	1.6 (0.66)	1.4 (0.67)	1.5 (0.98)	1.6 (0.89)	4.8 (0.08)	1.4 (1)

* Statistic error is about 5%.

Acetone represents an all purpose solvent, with α values ≥ 0.7 for all polymers.

Luminescence Decay Curves of **1** *and* **3b-7b** *in the Presence of Anthracene as Quenching Substrate*

To determine the accessibility of tethered ruthenium complexes for organic molecules, anthracene is added to the liquid phase of polymer suspensions. Energy transfer from the ^{3}MLCT excited state of the ruthenium complex to anthracene leads to the quenching of ruthenium luminescence. In solution, quenching results in the reduction of luminescence lifetimes, the decay curves remaining single exponential (Fig. 5). In the polymers, luminescence decay curves reveal two components, each representing a narrow distribution of decay curves with distinctly different mean decay times. The lifetime of the long component is approximately the same as the mean lifetime in the unquenched case. The lifetime of the short component decreases with increasing anthracene concentrations. From the luminescence decay curves the rate constants k_2 and accessibility factors α for the quenching process are calculated according to Eq. (7). In solutions of **1**, α = 1 is obtained, that is, all ruthenium complexes are equally accessible by anthracene (Table III). From the observed k_2 values, the quenching constants k_q are obtained by $k_q = k_2/c_A$, where c_A is the concentration of anthracene ($c_A = 5 \cdot 10^{-4}$ M). The quenching rate constants k_q are close to the diffusion rate constants k_d, which are calculated by $k_d = 4\pi N_A RD$, where N_A is Avogadro's number, R represents the encounter radius (R = 0.8 nm), and D is the diffusion coefficient of anthracene in the respective solvent. The fraction of successful encounters is found to be $k_q/k_d \approx 0.5 - 1$ for the solvents used in this study. In the polymeric materials, the kinetics of

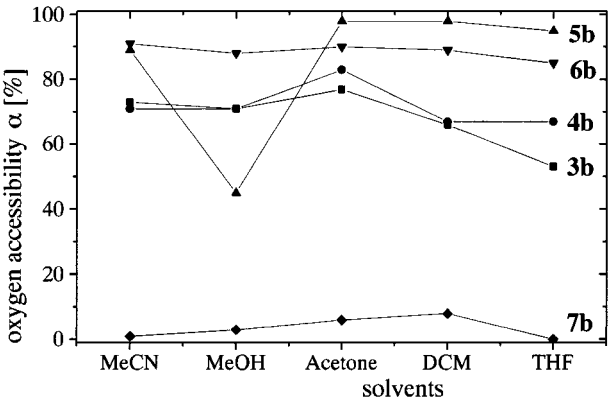

Fig. 4. Accessibility factor α for luminescence quenching by oxygen in the polymers **3b–7b**, suspended in a series of solvents. The values of α are obtained by evaluation of the corresponding luminescence decay curves according to Eq. (7).

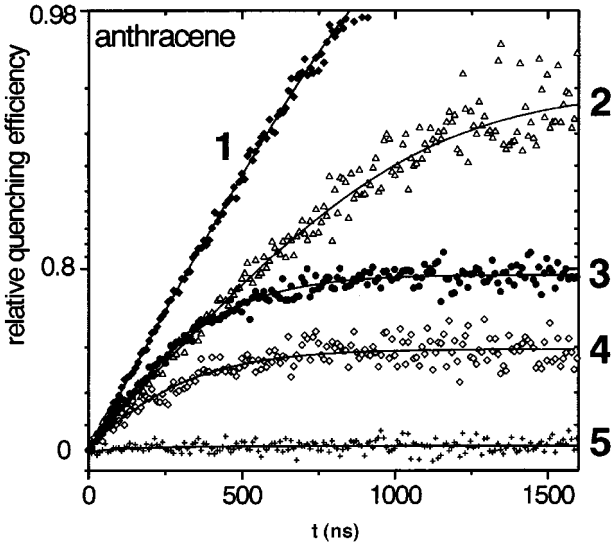

Fig. 5. Relative efficiencies, $1 - \frac{[R^*]}{[R^*]_{S=0}}$, for the quenching of ruthenium luminescence by anthracene. The curves are calculated from the corresponding luminescence decay curves according to Eq. (7). (1) **1** in dichloromethane solution, (2) **5b**, (3) **6b**, (4) **3b**, and (5) **7b**, suspended in dichloromethane. The concentration of anthracene in the liquid phases is c(anthracene) ≈ $5 \cdot 10^{-4}$ M.

Table III. Quenching Rate Constants, $k_2/10^6$ s^{-1}, and Accessibility Factors, α (in Parentheses), for the Luminescence Quenching by Anthracene (c(Anthracene) = $5 \cdot 10^{-4}$ M in the Liquid Phases) in Solutions of **1** and Suspensions of Polymers **3b–7b** in a Series of Solvents. The Values of k_2 and α are Obtained by Evaluation of the Corresponding Luminescence Decay Curves According to Eq. (7)

Sample Solvent	**3b**	**4b**	**5b**	**6b**	**7b**	**1**
MeOH	5.6 (0.80)	3.0 (0.62)	8.6 (0.45)	3.9 (0.78)	1 (0.22)	5.1 (1)
MeCN	3.8 (0.69)	7.0 (0.66)	3.4 (0.77)	8.6 (0.81)	— (0)	7.0 (1)
Acetone	4.6 (0.60)	4.4 (0.51)	3.2 (0.96)	5.3 (0.79)	6.3 (0.04)	5.1 (1)
THF	3.1 (0.46)	2.9 (0.50)	1.5 (0.88)	5.1 (0.69)	— (0)	9.4 (1)
DCM	4.6 (0.60)	9.9 (0.57)	3.2 (0.96)	5.1 (0.79)	6.3 (0.04)	5.1 (1)

* Statistic error is about 5%.

quenching by anthracene is in close analogy to the quenching by oxygen. Two kinds of ruthenium complexes can be distinguished. One of these populations is not quenched by anthracene, whereas the other one is quenched with the rate constant k_2. In the hybrid polymers **3b–7b** the k_2 values reach approximately 80–90% of the values observed for **1** in homogeneous solutions. Remarkably low values are observed for polymers suspended in THF. The absolute values of the accessibility factors α found for anthracene are slightly smaller than those observed for oxygen (Fig. 6 and Table III). However, the dependence of α on the type of polymer and the suspending liquid observed for anthracene and oxygen are similar. In the Q type material **7b**, the ruthenium complexes are practically not accessible by anthracene. Only in methanol the organic quencher reaches a significant fraction of complexes. In the polymers **3b** and **4b**, formed from bifunctional monomers, accessibilities vary between $\alpha \approx 0.4$ for less-polar solvents and $\alpha = 0.8$ for highly polar solvents. In polymer **6b**, accessibility factors are given by $\alpha \approx 0.7$–0.8, almost independent on the liquid phase. Maximum accessibilities of $\alpha \approx 0.9$–0.95 are achieved for polymer **5b** in solvents of low and medium polarity, whereas in acetonitrile and methanol only values of $\alpha \approx 0.8$ and $\alpha \approx 0.45$ are obtained, correspondingly.

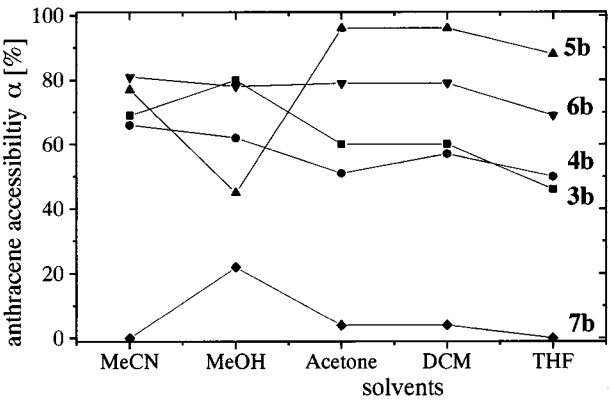

Fig. 6. Accessibility factor α for luminescence quenching by anthracene in the polymers **3b–7b**, suspended in a series of solvents. The values of α are obtained by evaluation of the corresponding luminescence decay curves according to Eq. (7).

CONCLUSION

The triethoxysilane modified ruthenium(II)-tris(bipyridyl) complex **2** was synthesized and sol-gel–processed with a series of different silane monomers to give the organically modified polysiloxanes **3b–7b**, which serve as model systems for inorganic–organic hybrid catalysts employed in hydrogenation and hydroformylation reactions. The materials were characterized by solid-state NMR spectra, BET measurements, elemental analysis, scanning electron microscopy, as well as steady-state and time-resolved luminescence spectroscopy. With the exception of polymer **4b**, all materials have small BET surface areas ($A < 5$ m^2/g). This result is supported by the absence of visible pores in SE micrographs. The appearances of the polymer particles in SE micrographs suggest that polymers **3b, 4b**, and **7b** are brittle particles with highly cross-linked three-dimensional structures, whereas **5b** is a soft material with low-dimensional cross-linking. Polymer **6b** shows an intermediate behavior.

Steady-state and time-resolved luminescence spectroscopy provides a detailed picture of the materials on the molecular level. Blue-shifted luminescence maxima and long luminescence decay times reveal that ruthenium complexes in the unmodified polysiloxane **7b** are solvated by a rigid solvation shell, and is probably formed by the polymer matrix itself. In contrast, ruthenium complexes in the organically modified polysiloxanes **3b, 4b**, and **6b** are preferentially solvated by the liquid phase. In the phenyl-modified polymer **5b**, the degree of solvation by the liquid depends strongly on the polarity of the liquid. Liquids of low and medium polarity provide high degrees of solvation; although highly polar, protic solvents such

as methanol do not even wet the particles. The non-exponential luminescence decay curves observed in all polymers indicate that complexes with distinctly different solvation conditions are existent.

Time-resolved studies of luminescence quenching by oxygen and anthracene reveal that the tethered ruthenium complexes can be divided into two populations. One of these populations is not accessible by the quenchers, whereas the other one is quenched with rate constants, which approach the values observed in homogeneous solutions. The accessibilities established for anthracene fall slightly below those obtained for oxygen, and this is mainly due to the larger size of the organic molecule. In the unmodified Q type material **7b**, the fraction of accessible ruthenium complexes is close to zero, irrespective of the suspending liquid. Solution-like accessibilities are found for the hybrid polymers **5b** and **6b** in solvents of low and medium polarity. In polar solvents, especially in methanol, the accessibility in the phenyl-containing polymer **5b** is poor because of reduced penetration of the polymeric networks by these solvents. In polar solvents, polymer **6b** and to a lesser extent polymers **3b** and **4b**, provide good accessibilities for both oxygen and anthracene.

These observations are in accordance with earlier results of NMR spectroscopic investigations on sol-gel–processed polysiloxanes, which show that Q-type materials possess a significantly higher degree of cross-linking than D- and T-type polymers [4]. On the other hand, the solvent dependence of the accessibilities in organically modified polymers reveals that the penetration of the polymer network by the solution of the quenchers in the liquid phase is not only determined by the degree of cross-linking but also by the compatibility of the solubility parameters of polymer and liquid phase.

ACKNOWLEDGMENTS

This work was supported by the Deutsche Forschungsgemeinschaft (Graduiertenkollge “Chemie in Interphasen” Grant. No. 441/01-2, Bonn-Bad Godesberg, Germany) and the Fonds der Chemischen Industrie, Frankfurt/Main. We thank E. Nadler (Institute for Physical Chemistry of the University of Tübingen), for SEM-, P. C. Schmidt and A. Brenn (Institute for Pharmacy of the University of Tübingen), for BET-, and S. Brugger (Institute for Inorganic Chemistry of the University of Tübingen), for NMR measurements.

REFERENCES

1. Supported Organometallic Complexes, Part 32. Part 31: Diaminediphenylphosphineruthenium(II) Precursor Complexes for Parallel Synthesis in Interphases E. Lindner, S. Al-Gharabli, and H. A. Mayer (2002) *Inorg. Chim. Acta* **334**, 113–121.
2. M. T. Murtagh, M. R. Shariari, and M. Krihak (1998) A study of the effects of organic modification and processing technique on the luminescence quenching behavior of sol-gel oxygen sensors based on a Ru(II) complex. *Chem. Mater.* **10**, 3862–3869.
3. M. A. Chan, J. L. Lawless, S. K. Lam, and D. Lo (2000) Fiber optic oxygen sensor based on phosphorescence quenching of erythrosin-B trapped in silica-gel glasses. *Anal. Chim. Acta* **408**, 33–37.
4. E. Lindner, F. Auer, T. Schneller, and H. A. Mayer (1999) Chemistry in interphases—A new approach to organometallic syntheses and catalysis. *Angew. Chem. Int. Educ. Engl.* **38**, 2154–2174.
5. J. H. Clark and D. J. Mcquarrie (1996) Environmentally friendly catalytic methods. *Chem. Soc. Rev.* **96**, 303–310.
6. E. Lindner, T. Schneller, H. A. Mayer, H. Bertagnolli, T. S. Ertel, and W. Hörner (1997) Hydrocarbon-bridged methyldimethoxysilanes as new co-condensation agents for the sol-gel process of the rhodium(I) complex $ClRh(CO)(P{\sim}O)_2$ containing the ligand $PhP(CH_2CH_2OCH_3)(CH_2)_3Si(OCH_3)$. *Chem. Mater.* **9**, 1524–1537.
7. E. Lindner, R. Schreiber, M. Kemmler, T. Schneller, and H. A. Mayer (1995) Solid-state NMR characterization of polysiloxane matrices functionalized with ether phosphines and their ruthenium(II) and palladium(II) complexes. *Chem. Mater.* **7**, 951–960.
8. B. Dunn, and J. I. Zink (1997) Probes of pore environment and molecule-matrix interactions in sol-gel materials. *Chem. Mater.* **9**, 2280–2291.
9. T. Keeling-Tucker and J. D. Brennan (2001) Fluorescent probes as reporters on the local structure and dynamics in sol-gel-derived nanocomposite materials. *Chem. Mater.* **13**, 3331–3350.
10. M. A. Meneses-Nava, O. Barbosa-Garcia, L. A. Diaz-Torres, S. Chavez-Cerda, and T. A. King (1999) Free volume effects on the fluorescence characteristics of sol-gel glasses doped with quinine sulfate. *Opt. Mat.* **13**, 327–332.
11. K. Maruszewski, M. Jasiorski, M. Salamon, and W. Strek (1999) Physicochemical properties of $Ru(bpy)_3^{2+}$ entrapped in silicate bulks and fiber thin films prepared by the sol-gel method. *Chem. Phys. Lett.* **314**, 83–90.
12. P. Innocenzi, H. Kozuka, and T. Yoko (1997) Fluorescence properties of the $Ru(bpy)_3^{2+}$ complex incorporated in sol-gel-derived silica coating films. *J. Phys. Chem. B* **101**, 2285–2291.
13. G. Hungerford, K. Suhling, and J. A. Ferreira (1999) Comparison of the fluorescence behaviour of rhodamine 6G in bulk and thin film tetraethylorthosilicate derived sol-gel matrices. *J. Photochem. Photobiol. A* **129**, 71–80.
14. L. M. Ilharco and J. M. G. Martinho (1999) Hybrid and nonhybrid silica sol-gel systems doped with 1,12-bis(1-pyrenyl)dodecane. *Langmuir* **15**, 7490–7494.
15. K. K. Flora, M. A. Dabrowski, S. P. Musson, and J. D. Brennan (1999) The effect of preparation and aging conditions on the internal environment of sol-gel derived materials as probed by 7 azaindole and pyranine fluorescence. *Canad. J. Chem. Rev. Canad. Chim.* **77**, 1617–1625.
16. C. D. Geddes, J. M. Chevers, and D. J. S. Birch (1999) Probing the sol-gel transition in SiO_2 hydrogels—A new application of near-infrared fluorescence. *J. Fluorescence* **9**, 73–80.
17. A. C. Franville, D. Zambon, R. Mahiou, and Y. Troin (2000) Luminescence behavior of sol-gel-derived hybrid materials resulting from covalent grafting of a chromophore unit to different organically modified alkoxysilanes. *Chem. Mater.* **12**, 428–435.
18. Y. Hou, A. M. Bardo, C. Martinez, and D. A. Higgins (2000) Characterization of molecular scale environments in polymer films by single molecule spectroscopy. *J. Phys. Chem. B* **104**, 212–219.
19. M. H. Huang, H. M. Soyez, B. S. Dunn, and J. Zink (2000) In situ fluorescence probing of molecular mobility and chemical changes

during formation of dip coated sol-gel silica thin films. *Chem. Mater.* **12**, 231–235.
20. S. M. Arabei, T. A. Pavich, J. P. Galaup, and P. Jardon (1999) Influence of the nature of sol-gel matrices on absorption and fine-structure fluorescence spectra of hypericin. *Chem. Phys. Lett.* **306**, 303–313.
21. D. S. Gottfried, A. Kagan, B. M. Hoffman, and J. M. Friedman (1999) Impeded rotation of a protein in a sol-gel matrix. *J. Phys. Chem. B* **103**, 2803–2807.
22. J.-L. Habib Jiwan, E. Robert, and J.-Ph. Soumillion (1999) Sol-gel silicate thin films bearing attached pyrene fluorescing probes hidden from oxygen but still accessible to organic electron transfer quenchers. *J. Photochem. Photobiol. A* **122**, 61–68.
23. M. Ogawa, T. Nakamura, J. Mori, and K. Kuroda (2000) Luminescence of tris(2,2′-bipyridine)ruthenium(II) cations ($[Ru(bpy)_3]^{2+}$) adsorbed in mesoporous silica. *J. Phys. Chem. B* **104**, 8554–8556.
24. U. Narang, R. A. Dunbar, F. V. Bright, and P. N. Prasad (1993) Chemical sensor-based on an artificial receptor element trapped in a porous sol-gel glass matrix. *Appl. Spectrosc.* **47**, 1700–1703.
25. R. C. Chambers, Y. Haruvy, and M. A. Fox (1994) Excited state dynamic in the structural characterization of solid alkyltrimethoxysilan-derived sol-gel films and glasses containing bound or unbound chromophores. *Chem. Mater.* **6**, 1351–1357.
26. P. B. Leezenberg, M. D. Fayer, and C. W. Frank (1996) Photophysical studies of probes bound to cross-link junctions in poly(dimethylsiloxane) elastomers and nanocomposites. *Pure Appl. Chem.* **68**, 1381–1388.
27. T. Suratwala, Z. Gardlund, K. Davidson, D. R. Uhlmann, J. Watson, and N. Peyghambarian (1998) Silylated coumarin dyes in sol-gel hosts. 1. Structure and environmental factors on fluorescent properties. *Chem. Mater.* **10**, 190–198.
28. S. Pandey, G. A. Baker, M. A. Kane, N. J. Bonzagni, and F. V. Bright (2000) On the microenvironments surrounding dansyl sequestered within class I and II xerogels. *Chem. Mater.* **12**, 3547–3551.
29. N. Leventis, I. A. Elder, Debra R. Rolison, Michele L. Anderson, and Celia I. Merzbacher (1999) Durable modification of silica aerogel monoliths with fluorescent 2,7 diazapyrenium moieties. Sensing oxygen near the speed of open-air diffusion. *Chem. Mater.* **11**, 2837–2845.
30. Ch. Malins, S. Fanni, H. G. Glever, J. G. Vos, and B. D. MacCraith (1999) The preparation of a sol-gel glass oxygen sensor incorporating a covalently bound fluorescent dye. *Anal. Commun.* **36**, 3–4.
31. A. H. O. Karkkainen, O. E. O. Hormi, and J. T. Rantala (2000) Covalent bonding of coumarin molecules to sol-gel matrices for organic light-emitting device applications. *Proc. SPIE-Int. Soc. Opt. Eng.* **3943**, 194–209.
32. J. C. Biazzotto, H. C. Sacco, K. J. Ciuffi, C. R. Neri, A. G. Ferreira, Y. Iamamoto, and O. A. Serra (1999) Synthesis of hybrid silicates containing porphyrins incorporated by a sol-gel process and their properties. *J. Non-Cryst. Solids* **247**, 134–140.
33. A. Lobnik, I. Oehme, I. Murkovic, and O. S. Wolfbeis (1998) pH optical sensors based on sol-gels: Chemical doping versus covalent immobilization. *Anal. Chim. Acta* **367**, 159–165.
34. T. Ishikawa, H. Inoue, and A. Makishima (1996) Optical properties of 1,4-dihydroxyanthraquinone covalently bonded to SiO_2-$AlO_{3/2}$ gel. *J. Non-Cryst. Solids* **203**, 43–48.
35. R. J. P. Corriu, P. Hesemann, and G. F. Lanneau (1996) Preparation and optical properties of hybrid sol-gel systems containing doubly anchored oligoarylenevinylenes. *Chem. Commun.* 1845–1846.
36. H.-J. Egelhaaf, E. Holder, P. Herman, H. A. Mayer, D. Oelkrug, and E. Lindner (2001) Synthesis, characterisation, and fluorescence spectroscopic mobility studies of fluorene labeled inorganic-organic hybrid polymers. *J. Mater. Chem.* **11**, 2445–2452.
37. M. Plaschke, R. Czolk, J. Reichert, and H. J. Ache (1996) Stability improvement of optochemical sol-gel film sensors by immobilisation of dye-labeled dextrans. *Thin Solid Films* **279**, 233–235.
38. For a series of papers on luminescent chemical sensors based on transition metal complexes, see: (2000). *Coord. Chem. Rev.* **205**, 3–228.
39. D. M. Roundhill (1994) *Photochemistry and Photophysics of Metal Complexes*. Plenum Press New York.
40. A. T. Yeh, C. V. Shank, and J. K. Mc Cusker (2000) Ultrafast electron localization dynamics following photo-induced charge transfer. *Science* **289**, 935–938.
41. N. Y. Turro (1978) *Modern Molecular Photochemistry*, Benjamin, Menlo Park.
42. A. Gilbert and J. Baggot (1991) *Essentials of Molecular Photochemistry*, Blackwell, Oxford.
43. A. Juris, V. Balzani, F. Barigelletti, S. Campana, P. Belser, and A. von Zelewsky (1988) Ruthenium(II) polypyridine complexes: photophysics, photochemistry, electrochemistry, and chemiluminescence. *Coord. Chem. Rev.* **84**, 85–277.
44. K. Kalyanasundaram (1992) *Photochemistry of Polypyridine and Porphyrin Complexes*, Academic Press, London.
45. D. L. Dexter (1953) A theory of sensitized luminescence in solids. *J. Chem. Phys.* **21**, 836–850.
46. E. Holder, G. Schoetz, V. Schurig, and E. Lindner (2001) Synthesis and enantiomer separation of a modified tris(2,2′-bipyridine)ruthenium(II) complex. *Tetrahedron. Asymmetry* **12**, 2289–2293.
47. D. A. Loy and K. J. Shea (1995) Bridged polysilsesquioxanes—highly porous hybrid organic-inorganic materials. *Chem. Rev.* **95**, 1431–1442.
48. L. L. Hench and J. K. West (1990) The sol-gel process. *Chem. Rev.* **90**, 33–72.
49. E. Lindner, R. Schreiber, T. Schneller, P. Wegner, H. A. Mayer, W. Gȍpel, and C. Ziegler (1996) Synthesis of polysiloxane-bound (ether phosphine)palladium complexes. Stoichiometric and catalytic reactions in interphases. *Inorg. Chem.* **35**, 514–525.
50. H. Laguitton-Pasquier, A. Martre, and A. Deronzier (2001) Photophysical properties of soluble polypyrrole-polypyridyl ruthenium(II) complexes. *J. Phys. Chem. B* **105**, 4801–4809.
51. H.-B. Kim, N. Kitamura, and S. Tazuke (1990) Time-dependent nonradiative decay in the metal-to-ligand charge transfer excited state of $Ru(bpy)_3^{(2+)}$. *J. Phys. Chem.* **94**, 7401–7405.
52. H.-J. Egelhaaf, B. Lehr, M. Hof, A. Hafner, M. Fritz, F. W. Schneider, E. Bayer, and D. Oelkrug (2000) Solvation and solvent relaxation in swellable copolymers as studied by time-resolved fluorescence spectroscopy. *J. Fluorescene* **10**, 383–392.
53. S. Draxler, M. E. Lippitsch, I. Klimat, H. Kraus, and O. S. Wolfbeis (1995) Effects of Polymer Matrixes on the Time-Resolved Luminescence of a Ruthenium Complex Quenched by Oxygen. *J. Phys. Chem.* **99**, 3162–3167.
54. P. Hartmann, M. J. P. Leiner, and M. E. Lippitsch (1994) Static and dynamic quenching of luminescent species in polymer media. *J. Fluorescence* **4**, 327–330.
55. M. T. Murtagh, H. C. Kwon, M. R. Shahriari, M. Krihak, and D. E. Ackley (1998) Luminescence probing of various sol-gel hosts with a Ru(II) complex and the practical ramifications for oxygen-sensing applications. *J. Mater. Res.* **13**, 3326–3331.
56. M. T. Murtagh, M. R. Shahriari, and M. Krihak (1998) A study of the effects of organic modification and processing technique on the luminescence quenching behavior of sol-gel oxygen sensors based on a Ru(II) complex. *Chem. Mater.* **10**, 3862–3869.
57. D. Garcia-Fresnadillo, M. D. Marazuela, M. C. Moreno-Bondi, and G. Orellana (1999) Luminescent nafion membranes dyed with ruthenium(II) complexes as sensing materials for dissolved oxygen. *Langmuir* **15**, 6451–6459.
58. C. J. Timpson, C. C. Carter, and J. Ohmsted III (1989) Mechanism of quenching of electronically excited ruthenium complexes by oxygen. *J. Phys. Chem.* **93**, 4116–4120.